Rapid near-infrared Raman spectroscopy system for real-time *in vivo* skin measurements

Zhiwei Huang and Haishan Zeng

Cancer Imaging Department, BC Cancer Agency, 601 West 10th Avenue, Vancouver, British Columbia V5Z 1L3, Canada

Iltefat Hamzavi, David I. McLean, and Harvey Lui

Division of Dermatology, University of British Columbia and Vancouver General Hospital, 835 West 10th Avenue, Vancouver, British Columbia V5Z 4E8, Canada

Received June 25, 2001

A rapid dispersive-type near-infrared (NIR) Raman spectroscopy system and a Raman probe were developed to facilitate real-time, noninvasive, *in vivo* human skin measurements. Spectrograph image aberration was corrected by a parabolic-line fiber array, permitting complete CCD vertical binning, thereby yielding a 3.3–16-fold improvement in signal-to-noise ratio. Good quality *in vivo* cutaneous NIR Raman spectra free of interference from fiber fluorescence and silica Raman scattering can be acquired in less than 1 s, which greatly facilitates practical noninvasive tissue characterization and clinical diagnosis. © 2001 Optical Society of America

OCIS codes: 170.5660, 170.6510, 170.1870.

Raman spectroscopy is a unique analytic probe for molecular vibrations and may provide specific information about the structure and conformation of biomolecular constituents in tissues.[1,2] Clinical applications have been limited not only by the difficulty in capturing the inherently weak tissue Raman signals but also by the relatively slow speed of spectral acquisition. Fourier-transform Raman systems typically require as long as 30 min to acquire spectra from *ex vivo* tissue samples.[3] For clinical uses, Raman measurements should be performed *in vivo* and quickly, preferably within seconds or subseconds. Based on recent technical advances in high-sensitivity CCDs, high-throughput holographic spectrographs, and compact diode lasers, a number of groups have developed compact dispersive-type Raman systems for acquiring *in vivo* tissue spectra.[4–6] In this Letter we present a unique method for improving the signal-to-noise (S/N) ratio and the spectral resolution of a Raman spectrometer by correcting the spectrograph's image aberration. Good quality near-infrared (NIR) Raman spectra can be acquired from *in vivo* human skin in less than 1 s, paving the way for practical Raman data collection in the clinical setting.

The Raman system consists of an external-cavity stabilized diode laser (785 nm, 300 mW; Model 8530, SDL), a transmissive imaging spectrograph (HoloSpec-$f/2.2$-NIR, Kaiser), a NIR-optimized, back-illuminated, deep-depletion, CCD detector (LN/CCD-1024EHRB, Princeton Instruments), and a specially designed Raman probe. The laser is coupled to our Raman probe via a 200-μm core-diameter fiber. Tissue-scattered Raman photons are collected from the probe by a fiber bundle and fed into the spectrograph, whereupon the photons are dispersed onto the CCD array detector by a volume-phase technology holographic grating. A PC controls the CCD detector and the spectral data acquisition, processing, and display. The CCD, with enhanced quantum efficiency and reduced etaloning in the NIR (quantum efficiency, $\geq$75% at 900 nm), was liquid-nitrogen cooled, and its S/N ratio was readout noise limited when weak Raman signals were acquired. The CCD consisted of 1024 $\times$ 256 pixels (27 μm $\times$ 27 μm) and allowed vertical binning for improved detection sensitivity. The spectrograph's f-number of 2.2 exactly matched the N.A. of the fiber bundle (N.A., 0.22), which in turn provided five times better throughput than traditional $f/4$, quarter-meter imaging Czerny–Turner spectrographs used in conventional dispersive Raman systems.[7] The whole system was packed onto a movable cart for outpatient clinical data acquisition.

We designed the Raman probe to maximize the collection of tissue Raman signals while reducing the interference of Rayleigh-scattered light, fiber fluorescence, and silica Raman signals. The probe consisted of two arms, as shown in Fig. 1. A 0.5-in.- (1.27-cm-) diameter optics illumination arm that incorporated a collimating lens, a bandpass (BP) filter (785 $\pm$ 2.5 nm), and a focusing lens delivered the laser light onto the skin surface, with a spot size of 3.5 mm. A 1-in.- (2.54-cm-) diameter optics collection arm with collimating and refocusing lenses and a holographic notch plus filter (optical density, >6.0 at 785 nm; Kaiser) was used for collecting Raman emissions. The collimating lens was positioned so that its focal point was located at the skin surface, leading to a collimated beam between the two lenses. We placed a notch filter between the two lenses to block the backscattered laser light and pass the frequency-shifted Raman signal. A refocusing lens then focused the filtered beam onto the circular end of the fiber bundle. The collection arm was perpendicular to the skin surface,

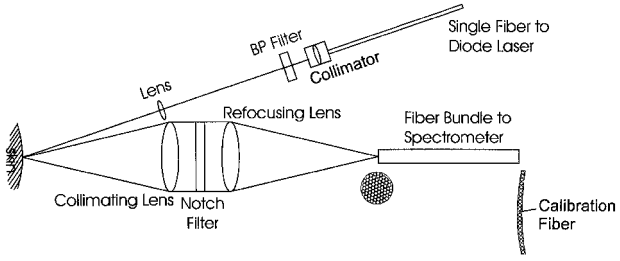

Fig. 1. Optical layout of the skin Raman probe.

0146-9592/01/221782-03$15.00/0 © 2001 Optical Society of America

and we placed the illumination arm at a 40° angle to avoid collection of specularly reflected laser light. We mounted all optical components in a rigid metal case to keep them in the desired positions.

To enhance the detection of the inherently weak Raman signals, we packed as many fibers into the fiber bundle as allowed by the CCD height (6.9 mm). The fiber bundle consisted of 58 100-μm fibers arranged in a circular shape at the input end of the probe and a linear array at the output end that was connected to the spectrograph's entrance (Fig. 1). Another 50-μm fiber was placed at the center of the output linear array and split out of the bundle for wavelength calibration. At the circular end the fibers were packed into a 1.6-mm-diameter area, which also defined the measurement spot size at the skin surface.

It is well known that the image of a straight slit through any spectrograph utilizing a plane grating has a curved shape that is usually parabolic.[8] This image aberration arises from the fact that rays from different positions along the length of the slit are incident on the grating at varying degrees of obliqueness. For spectrographs with short focal lengths, this obliqueness causes significant distortion that can affect the measurement performance of the detector. Figure 2A shows the image aberration of a 100-μm slit through the spectrograph in our uncorrected system when it is illuminated by a mercury argon lamp. The curvature of the spectral lines is apparent, and in Fig. 3 the horizontal displacement of a spectral line from Fig. 2A is shown graphically, with the displacement rounded to pixels (dashed lines). The maximum horizontal displacement is 5 pixels (135 μm). The solid line is a linear regression-fitted parabolic curve described by $x = 1.1904 \times 10^{-5}y^2 + 1.9455 \times 10^{-4}y - 0.98613$, where x is the horizontal displacement at a vertical position, y.

This image aberration causes two problems for hardware binning of CCD columns: (1) It decreases the spectral resolution and (2) it decreases the S/N ratio that is achievable otherwise. It also causes problems with wavelength calibration. Hardware binning is CCD binning performed before signal readout by the preamplifier. For signal levels that are readout-noise limited, for instance, for weak Raman signal measurements, hardware binning improves the S/N ratio linearly with the number of pixels grouped together.[9] For signal levels that are shot-noise limited, hardware binning improves the S/N ratio by only the square root of the number of pixels grouped together. Binning can also be done by use of software after the signal is read out. However, software binning improves the S/N ratio by only as much as the square root of the number of pixels added together.[10] Hence, complete hardware binning of the entire vertical line is preferable for maximizing the S/N ratio. To date, we know of no effort to correct this image aberration. The manufacturer (Kaiser) of the HoloSpec spectrograph suggested binning the 11 segments shown in Fig. 3 separately by use of hardware binning and then shifting the appropriate number of pixels before summing them together with software.[8] We call this a combined hardware and software binning procedure. Another method is to acquire the whole image first and then add all the pixels along the curve together with software. We call this a complete software binning procedure.

We conceived a simple but novel solution for dealing with this image aberration. As shown in Fig. 1, we aligned the 58 fibers of the fiber bundle at the spectrograph's end along a curve formed by laser drilling of a stainless-steel cylinder piece,[11] the shape of which corresponded directly to the horizontal displacement shown in Fig. 3 but in the reverse orientation. Figure 2B shows a CCD image of the fiber bundle illuminated by a mercury argon lamp. The central dark spots in the spectral lines are from the calibration fiber that was not illuminated. With this specific fiber arrangement the spectral lines are substantially straight, indicating effective image-aberration correction, which in turn allows us to completely bin the entire CCD vertical line (256 pixels) without losing resolution and reducing the S/N ratio. Therefore the S/N ratio improvement that we achieve with our system could be up to a maximum value of $11/\sqrt{11} = \sqrt{11} = 3.3$ times that of the combined hardware and software binning procedure[8] and $256/\sqrt{256} = \sqrt{256} = 16$ times that of the complete software binning.

The system covered a spectral range 800–1800 cm^{-1}. Raman frequencies were calibrated with

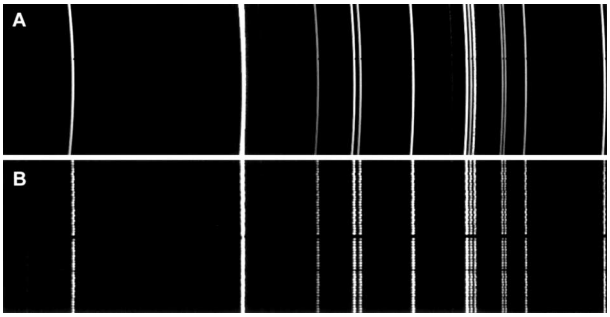

Fig. 2. (a) Image of a 100-μm slit on the CCD through the HoloSpec spectrograph, demonstrating the image aberration. (b) CCD image of 58 fibers aligned along a parabolic line at the entrance of the spectrograph, demonstrating that the image aberration has been corrected from (a).

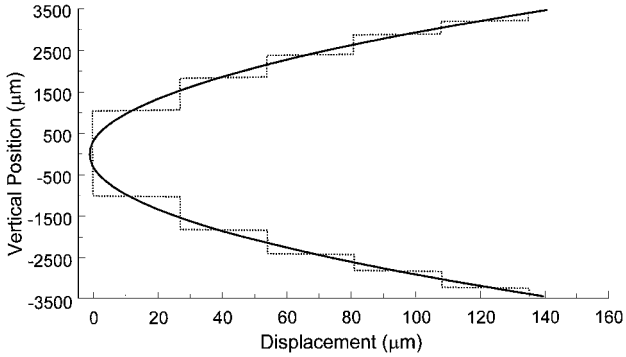

Fig. 3. Graphic representation of the curve observed in Fig. 2A, showing the horizontal displacement rounded to pixels (dashed lines). The solid curve is a linear-regression-fitted parabolic line.

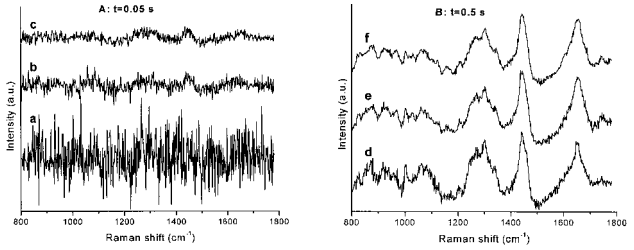

Fig. 4. Comparison of *in vivo* Raman spectra from healthy palm skin obtained in three different acquisition modes and at two different CCD exposure times: A, $t = 0.05$ s; B, $t = 0.5$ s. Curves a and d are from the complete software binning mode, b and e are from the combined hardware and software binning mode, and c and f are from the hardware binning mode.

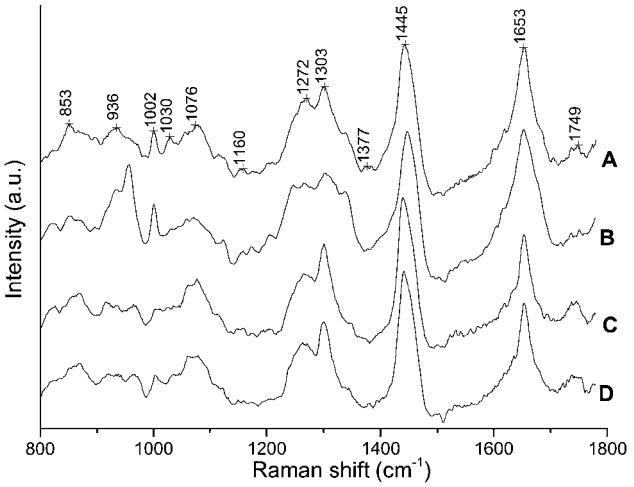

Fig. 5. Examples of *in vivo* skin Raman spectra obtained from various body locations of a healthy volunteer. A, palm of the hand; B, fingernail; C, surface of the forearm; D, volar aspect of the forearm.

cyclohexane, acetone, and barium sulfate to an accuracy of ± 2 cm^{-1}, and the spectral resolution was 8 cm^{-1}. All spectra acquired were corrected for the spectral sensitivity of the system by use of a standard lamp (RS-10, EG&G Gamma Scientific). We used a fifth-degree polynomial[9] to fit the background tissue autofluorescence in the measured raw data, and we then subtracted this polynomial from the measured spectrum to obtain the tissue Raman signals.

The *in vivo* skin Raman measurements made with our system in hardware binning mode can be obtained in less than 1 s, and some Raman peaks are discernible even with an exposure time of 0.01 s. The illumination power density is 1.56 W/cm^2, less than the ANSI maximum permissible skin exposure limit of 1.63 W/cm^2 for a 785-nm laser beam.[12] Figure 4 shows Raman spectra from a human palm under complete software binning (curves a and d), combined hardware and software binning (curves b and e), and hardware binning (curves c and f) acquisition modes with CCD integration times of 0.05 s (Fig. 4A) and 0.5 s (Fig. 4B), respectively. In both Figs. 4A and 4B, the S/N ratio of the spectra obtained with hardware binning is better than that obtained with the combined hardware and software binning and much better than that of complete software binning. The signals in Fig. 4A are readout-noise limited. The binned original signals (fluorescence plus Raman) corresponding to Fig. 4B are of the order of 2400 to 15,000 counts, and the CCD well depth facilitates a maximum signal of 65,535 counts before saturation. The signal at each pixel is, therefore, of the order of 9 (2400/256) to 59 (15,000/256) counts, closing to a readout-noise-limited situation and far from a shot-noise-limited situation.

Figure 5 shows examples of *in vivo* Raman spectra of different skin locations from a healthy volunteer. All specta were obtained with an integration time of 0.5 s. For comparison, all spectra were normalized to 1 at 1445 cm^{-1}. The prominent vibrational features of human skin, such as the ν (C=O) amide I band at 1654 cm^{-1}, the δ (CH_3) and δ (CH_2) scissoring mode at 1445 cm^{-1}, the CH_2 deformation at 1301 cm^{-1}, and the ν (CN) and δ (NH) amide III bands at 1269 cm^{-1}, can be clearly discerned in all spectra and are consistent with the Fourier-transform Raman spectra of skin reported in the literature.[2,3,13]

In conclusion, an image-aberration-corrected rapid NIR Raman spectroscopy system and a special skin Raman probe have been designed, constructed, and evaluated. The successful acquisition of Raman spectra from human skin *in vivo* in less than 1 s presents great potential for skin tissue characterization at the molecular level and noninvasive medical diagnosis.

This research was supported by the National Cancer Institute of Canada and the Canadian Dermatology Foundation. H. Zeng's e-mail address is hzeng@bccancer.bc.ca.

References

1. A. Mahadevan-Jansen and R. Richards-Kortum, J. Biomed. Opt. **1,** 31 (1996).
2. B. W. Barry, H. G. M. Edwards, and A. C. Williams, J. Raman Spectrosc. **23,** 641 (1992).
3. H. G. M. Edwards, A. C. Williams, and B. W. Barry, J. Mol. Struct. **347,** 379 (1995).
4. M. G. Shim, L. K. Song, N. E. Marcon, and B. C. Wilson, Photochem. Photobiol. **72,** 146 (2000).
5. J. J. Baraga, M. S. Feld, and R. P. Rava, Appl. Spectrosc. **46,** 187 (1992).
6. A. Mahadevan-Jansen, M. F. Mitchell, N. Ramanujam, U. Utzinger, and R. Richards-Kortum, Photochem. Photobiol. **68,** 427 (1998).
7. H. Owen, D. E. Battey, M. J. Pelletier, and J. B. Slater, Proc. SPIE **2406,** 260 (1995).
8. HoloSpec VPT System Operations Manual, Kaiser Optical Systems, Ann Arbor, Mich., 1994.
9. ST-133 Controller Operations Manual, Princeton Scientific Istruments, Monmouth Junction, N.J., 1997.
10. A. Mahadevan, N. Ramanujam, M. F. Mitchell, A. Malpica, S. Thomsen, and R. Richards-Kortum, Proc. SPIE **2388,** 110 (1995).
11. H. Zeng, "Apparatus and methods relating to high speed Raman spectroscopy," U.S. patent pending.
12. "American National Standard for the Safe Use of Lasers," ANSI Standard 2136.1-1986 (American National Standards Institute, Washington, D.C., 1986).
13. P. J. Caspers, G. W. Lucassen, R. Wolthuis, H. A. Bruining, and G. J. Puppels, Biospectroscopy **4,** S31 (1998).